

Inverse Heat Flux Evaluation using Conjugate Gradient Methods from Infrared Imaging

by J. Sousa*, L. Villafane*, S. Lavagnoli*, and G. Paniagua*

*Turbomachinery & Propulsion Dep., von Karman Institute, Rhode-Saint-Genèse, Belgium, jorge.sousa@vki.ac.be

Abstract

Inverse heat conduction is generally associated with the estimation of unknown boundary heat fluxes on an inaccessible surface from temperature measurements performed on the accessible wall. In the present application temperature measurements using infrared thermography on 3D surfaces were performed in combination with an inverse heat conduction method. In this study the 3D transient inverse heat conduction problem was solved using conjugate gradient methods (CGM), coupled with a finite element (FE) commercial solver. The input of this model was provided by infrared thermal imaging measurements used to monitor the temperature evolution of an accessible wall. The efficiency of the method was demonstrated through numerical simulations and validated in a simplified experimental setup.

1. Introduction

The knowledge of surface thermal loads is of paramount importance to develop innovative propulsion designs and extend the information of the heat transfer phenomena through complex geometries. Typical measurement techniques use direct surface temperature data to compute the wall heat flux [1]. The data reduction is simplified by considering 1D and semi-infinite heat transfer assumptions. However, most engine components are geometrically complex and these assumptions are not valid and furthermore, direct optical access might not be available. New experimental and data reduction techniques based on inverse methods must be developed to model the 3D effects and to eliminate the requirement of direct optical access. Since the knowledge of spatial surface temperature in the accessible wall is necessary, thermal imaging is preferred to discrete measurements provided by thermocouples.

Inverse problems are mathematically *ill-posed*, in contrast with direct heat transfer problems that are considered as *well-posed* [2]. For this reason inverse problems are very sensitive to measurements errors requiring therefore regularization techniques to reach a stable solution. Applications of these methods to 1D and 2D geometries are commonly found in literature [2], [3]. The solutions of the heat transfer equation are usually based on analytical expressions or on finite differential methods where the inverse problem is solved by means of regularization or minimization methods [5]. Transient three dimensional inverse problems with irregular domain are scarce in the open literature. At Onera [4], a sequential method was implemented to solve a three dimensional problem in regular domains. An alternative producer using classic conjugate gradient method was implemented by C. H. Huang [6]. The inverse algorithm was coupled with a numerical solver where irregular domains could be solved. All the techniques employed to deal with inverse heat transfer problems are based on finite differential methods solved with optimization algorithms and regularization methods. A detailed overview on the possible optimization and regularization methods associated with inverse thermal problems is performed in [7]. Conjugate gradient methods are presented as a minimization technique that several authors [6], [8] consider a robust method to solve inverse heat conduction problems.

The objective of the present research was to estimate the wall heat flux on an inaccessible wall of a three dimensional domain from the knowledge of the surface temperatures in an opposite wall to the boundary of interest. The conjugate gradient method was applied with the adjoint problem [9]. The three dimensional heat transfer equation was solved with a commercial code *COMSOL* working as a sub-routine of the inverse algorithm. This link allows to model complex geometries with different boundary and initial conditions.

The sensitivity and application range of the method was provided by its numerical and experimental validation. Following Woodbury [10] the validation was performed by imposing different heat fluxes with square and triangle temporal shapes. Different non-dimensional thickness, noise ratio, and geometries are also studied. Experimental validation was performed by imposing a heat flux on the back side wall and measure the temperature with the infrared camera on the opposite wall. The estimated temperature was then compared with the imposed one by means of a second infrared camera.

2. Description of the method

This paper proposes the use of a deterministic and stochastic technique [8] to solve the inverse heat transfer problem. The method makes use of minimization techniques similar to those used in optimization problems, where the objective function R is defined by Eq.(1).

$$R[\dot{q}(S, t)] = \sum_{t=0}^{tf} \sum_{m=1}^M (T_m(t) - Y_m(t))^2 \quad (1)$$

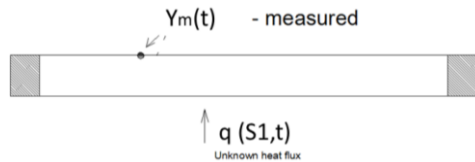


Fig. 1 Inverse heat conduction problem

The objective function involves the squared difference between measured temperature $Y_m(t)$ with infrared thermography and the estimated temperature $T_m(t)$ computed with the direct problem by imposing the estimated heat flux $\dot{q}(S, t)$. Where tf represents the final time and M the total number of measurement points on the surface S , this value represents the number of pixel of the infrared image that is a function of the spatial resolution.

2.1. Conjugate Gradient methods

The CGM is an iterative method that should converge to a minimum of the objective function. At each iteration Eq. (2) was used to compute the estimated heat flux $\dot{q}(S, t)$ where β the search step size, P the direction of descent and n the iteration number.

$$\dot{q}^{n+1}(S, t) = \dot{q}^n(S, t) - \beta^n P^n(S, t) \quad (2)$$

This method chooses a direction of descent that is a linear combination of the gradient direction $J(S, t)$ with the direction of descent of the previous iteration based on the following equation:

$$P^n(S, t) = J^n(S, t) + \gamma^n P^{n-1}(S, t) \quad (3)$$

Different versions of conjugate gradient methods can be used to compute the conjugation coefficient γ , [8]. In the implemented method, γ was computed from

$$\gamma^n = \frac{\sum_{t=0}^{tf} \sum_{m=1}^M (J^n)^2}{\sum_{t=0}^{tf} \sum_{m=1}^M (J^{n-1})^2} \quad (4)$$

In order to perform the iterative process let us first compute the step size β and the gradient of descent $J(S, t)$ by making use of the sensitivity and adjoint problems [6]. The search step size is obtained with the solution of the sensitivity problem. The problem is defined as the directional derivative of the direct problem in the direction of the perturbation of the unknown function. The direction of descent $J(S, t)$ is obtained by solving the adjoint problem. For this a Lagrange multiplier is used in the minimization of the function R . Both of these problems can be transformed in a simple three dimensional Fourier law problem by specifying correctly the boundary and initial conditions. As performed in [6] this allows to obtain the solution of each problem with a finite element solver without changing the implemented equations. For further details of these auxiliary problems, the reader is referred to [6], [9], [10].

2.1. Stopping criteria

When the experimental measured data has random errors they are amplified in the solution when the minimum of function R is reach, resulting in an unstable solution. In order to avoid this, the iterative process is stopped when the objective function reaches a certain minimum level.

$$R(q(S, t)) < \varepsilon \quad (5)$$

The tolerance value ε is determined based on the idea that discrepancies between the measured data Y_m and the computed one T_m cannot not be smaller than the uncertainty of the infrared measurements. In the present case the discrepancy principle is used to compute this value [8]. This principle assumes that the final solution of the inverse method is sufficiently accurate when the difference between estimated and measured temperatures is on the order of the standard deviation σ of the infrared measurements.

$$\varepsilon = M\sigma^2 t_f \quad (6)$$

Where M is the total number of measured points, t_f the final time and σ the standard deviation of the infrared measurements.

2.2. Computational methodology

The methodology requires the solution of the direct, sensitivity and adjoint heat conduction problem through the solid, therefore a commercial available FE solver (COMSOL) was used for this purpose. A generalized 3D inverse heat transfer problem was implemented based on *the LiveLink[™] Matlab[®]* environment. The combination of a numerical solver with the inverse method allowed to model complex geometries and all kinds of boundary and initial conditions. The computational methodology is illustrated in figure 2.

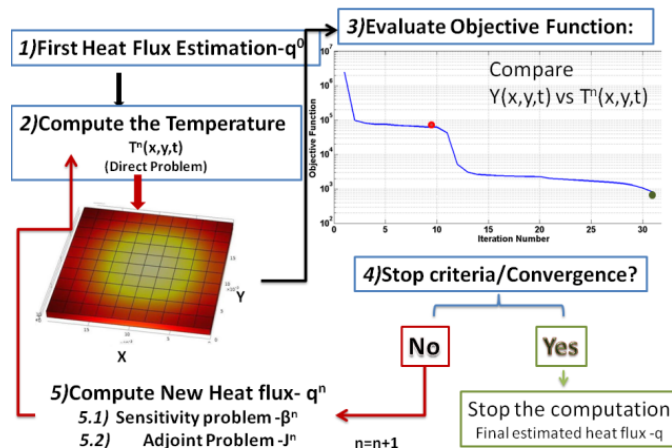


Fig. 2 Illustration of the computational methodology

The direct problem is computed based on a random first estimation of $q^0(x, y, t)$, therefore, the present method does not require any initial information of the unknown heat flux. Afterwards $T^n(x, y, t)$, on the opposite wall, is obtained through the 3D FE solver with the previous referred boundary condition. By comparing this temperature with the measured one, $Y(x, y, t)$, the objective function is evaluated. If the stopping criterion is not reach the new heat flux is computed by solving the sensitivity and adjoint problem. This process is iterated until the stopping criterion is satisfied.

3. Numerical Validation

The objective of the numerical validation was to prove the validity of the present method to solve a generalized transient inverse method applied to 3D geometries. The wall heat flux $q(S1, t)$ was estimated from the knowledge of the transient temperature on the opposite surface. The first step of the validation was to impose a known heat flux on the *virtual* inaccessible wall of the 3D geometry and *measure* the temperature evolution on the accessible wall. This temperature was then the input for the inverse method. Finally the estimated heat flux was compared with the imposed one.

Several studies were performed to validate and understand the sensitivity of the method to different experimental situations. In order to mimic the results for cases involving random measurement errors, artificial noise was added on the measured temperature. Furthermore, different geometries were tested. The simulated setup consists of a rectangular geometry with adiabatic lateral walls. Its characteristics are summarized in table 1

Table 1 Physical and geometric characteristics of the numerical model

Conductivity k (W/mK)	63.9
Density ρ (kg/m ³)	7854
Capacity C (J/kgK)	434
Width (m)	0.002
Thickness L (m)	0.001;0.005;0.010

3.1.1. Square and triangle heat flux

The first test consists in prescribing a heat flux that was spatial uniformly distributed, with a square and triangular temporal shape evolution. The steep imposed heat flux represents a strict way to evaluate the accuracy and stability of the implemented method. The first test was performed assuming exact measurements for different dimensionless thicknesses defined by the heat penetration depth ($\tilde{L} = L/3.74\sqrt{\alpha\Delta t}$), where Δt is the time that the heat flux was imposed on the surface. Figure 3 exhibits the estimated and the imposed heat flux evolution in function of the dimensionless time ($\xi = \alpha t/L^2$).

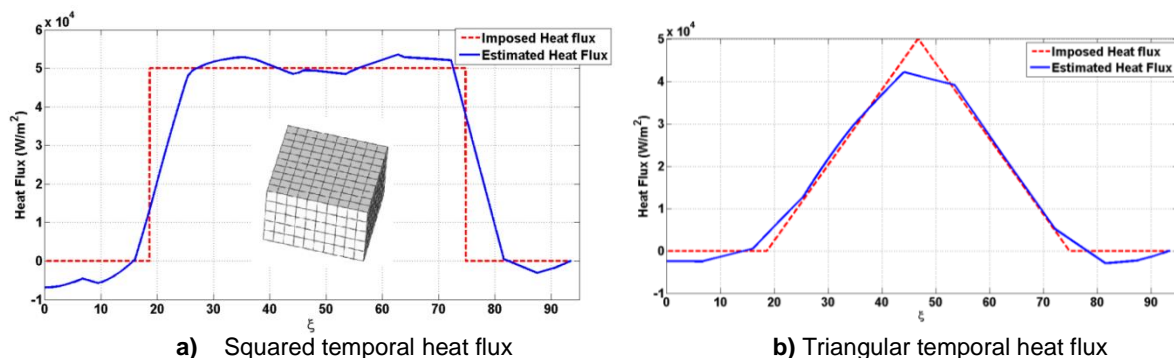


Fig. 3 Numerical validation for steep heat flux gradients

The converged solution was obtained after 80 and 45 iterations for a squared and triangular shape respectively. The solution shows a poor prediction for the locations with discontinuities in the heat flux. The average error of both of the cases was 5% and 2% respectively. The average error was computed with Eq. (7)

$$AV_{error} = \sum_{m=1}^M \sum_{t=0}^{t_f} \frac{q(S, t) - \hat{q}(S, t)}{\hat{q}(S, t)_{max}} \quad (7)$$

Where $\hat{q}(S, t)$ and $q(S, t)$ are the estimated and exact heat flux. S is the surface of the unknown heat flux. The solution close to the discontinuities might be improved by increasing the number of iteration but mainly by reducing the time step of the computations at the price of increased computational time.

3.2. Sensitivity of the model to noise level and thermal thickness

The influence of the measurement noise on the inverse model was assessed by adding to the measured temperature artificial noise, with zero mean and constant standard deviation. The noise influence was analyzed for three different levels. For each case the stopping criteria has to be re-adapted according to Eq(6). The estimated heat fluxes are plotted on figure 4.

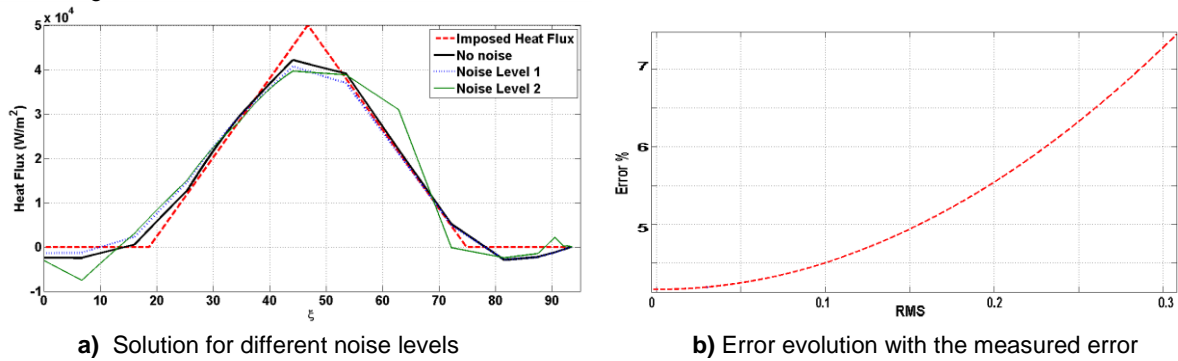


Fig. 4 Estimated solution for different noise level

The standard deviation for the noise level 1 and 2 were respectively 0.05 and 0.3 with an average error of 4 and 6.9%. These results show that a reliable estimation of the heat flux can still be obtained in the presence of noisy measurements however with an increase on average error of the final solution.

The influence of the dimensionless thickness, \bar{L} , was analyzed by means of a parametric study. This parameter quantifies how much the heat transfer is damped by conduction through the solid. This value is a function of the thickness L , of the solid and total time of imposed heat flux, Δt . Figure 5 shows the evolution of the average error in function of the dimensionless thickness.

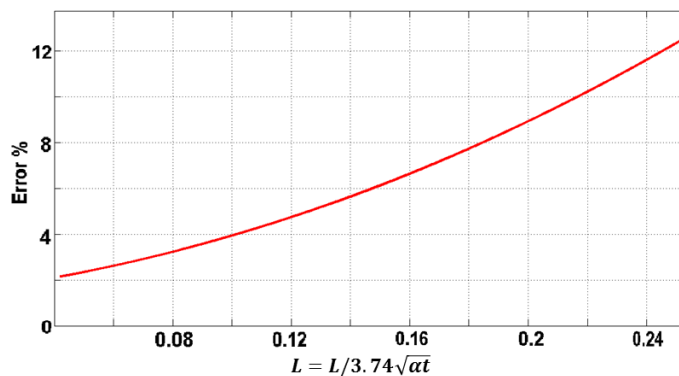


Fig. 5 Evolution of the average error with the thermal thickness

The average error increases with the thickness or with the decrease of the time with imposed heat flux Δt . This analysis shows that larger thickness can still be resolved as long as there is enough time for the information to travel by conduction through the solid.

3.3. Boundary conditions of the numerical model

The walls where the infrared measurements are performed are not adiabatic and thus the measured temperature is not just a function of the unknown heat flux, it also depends on the convective and radiative losses in that surface, as illustrated in figure 6. If the convective heat transfer coefficient h , the ambient temperature T_{amb} and the surface emissivity ϵ can be properly predicted, these losses can be taken into account during the inverse computation by superimposing these boundary conditions. The heat flux can still be recovered with acceptable accuracy.

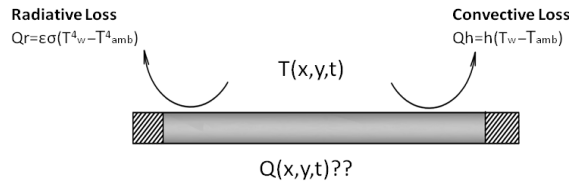


Fig. 6 Illustration of the convective and radiative loss on the measured wall

The present method also allows to impose a known boundary condition on the lateral walls, which is a requirement to solve a full 3D model. Initial boundary conditions can also be prescribed for cases where the transient phenomena start with non-uniform temperatures along the domain. This can be achieved by obtaining primarily the steady state solution and using this result as an initial condition for the transient heat transfer.

3.4. Results for a spatial distributed heat flux

A test case with a transient spatial distributed heat flux was performed for a flat plate. Each square illustrated on the surface of the plate represents a pixel of the infrared image. The exact heat flux is characterized by a radial distribution and a temporal sinusoidal shape. Figure 7 exhibits on the left the imposed heat flux, at a certain time, and on the right side the estimated heat flux after 70 iterations.

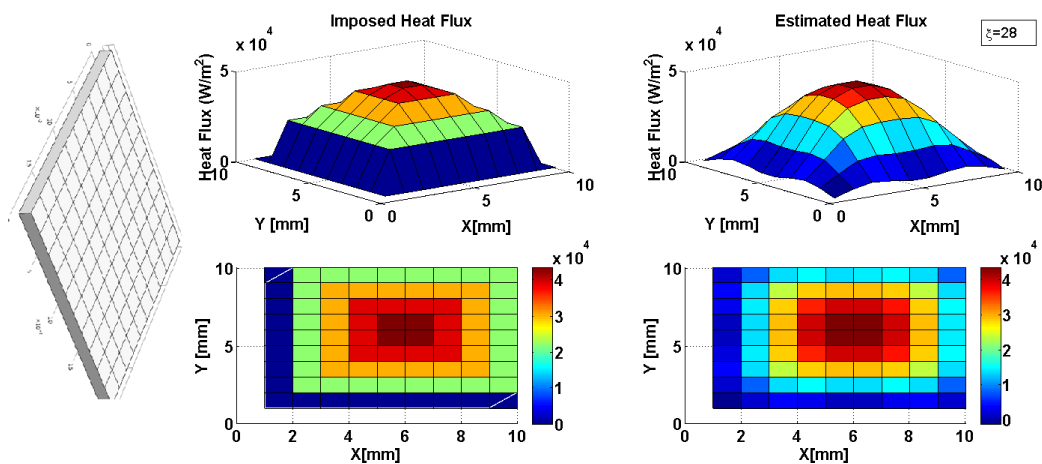


Fig. 7 Exact (left) and estimated (right) for a radial distributed heat flux

This test was evaluated for two different thicknesses $L=0.036$ and 0.107 providing an average error about 7% and 9% respectively.

4. Experimental Validation

4.1. Set up and methodology

Experimental validation of the numerical method was performed in a simplified set up. The model considered was a plate and its characteristics are resumed in table 2.

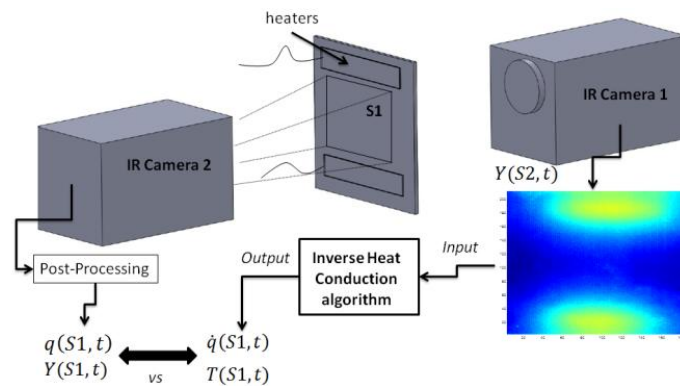
Table 2 Characteristics of the experimental model

Conductivity k	(W/mK)	172
Density ρ	(kg/m ³)	2700
Capacity C	(J/kgK)	894
Width	(m)	0.2
Thickness L	(m)	0.005

The experimental set up is illustrated in figure 8. Two infrared cameras and four thermocouples were used to measure the temperature time series on both sides of the plate.

A heat flux (q) was imposed on one of the surface ($S1$) and the temperature ($Y(S1, t)$) evolution, on the same surface, was measured by the Infrared camera 2 (*FLUKE Ti50FT*). On the opposite surface ($S2$) the temperature ($Y(S2, t)$) was monitored by the infrared camera 1 (*FLIR SC3000*). The measured temperature on this surface was the input for the implemented method.

The objective was to estimate the heat flux on surface $S1$. Finally the temperature measured by camera 2 was compared with the IHCM results. The heat flux was imposed by means of electrical heaters. Two thermocouples are bounded to each side of the surface in order to perform single point calibrations of the IR cameras and the time series validation.



4.2. Preliminary Results and discussion

The first step to solve the inverse heat conduction problem is to model the physical domain and impose the proper known boundary conditions. For the experimental case presented, the unknown heat flux was imposed by the electrical heaters placed close to the top and bottom boundaries of the physical domain, figure 8. Natural convection was imposed as a boundary condition on the opposite surface where the temperature was measured (S2) as well as the on the lateral walls.

The test was started with the heaters turned off and the model in a steady state at ambient temperature. Several seconds after the acquisition is started, the heaters were turned on and a constant heat flux was imposed by setting a constant voltage.

In the first phase of the validation, the spatial resolution of camera 1 was reduced ten times in order to decrease the computational time (due to data transfer between the two codes). However most of the spatial information of the temperature distribution was kept as shown in figure 9.

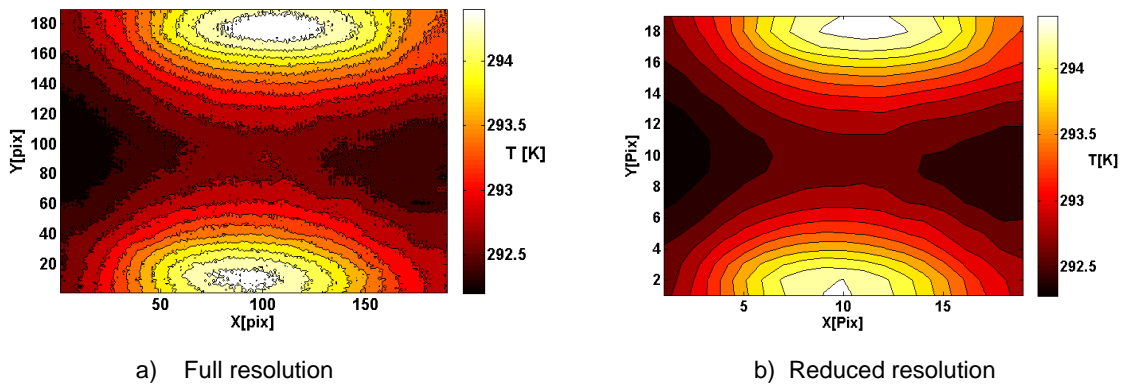


Fig. 9 Temperature field $Y(S2, t_n)$ on surface S2

The measured temperature on surface S2 (19 by 19 points) was the input for the IHCM in which 160s of heat flux was considered. The solution of the inverse problem is plotted in figure 10 obtained after 19 iterations.

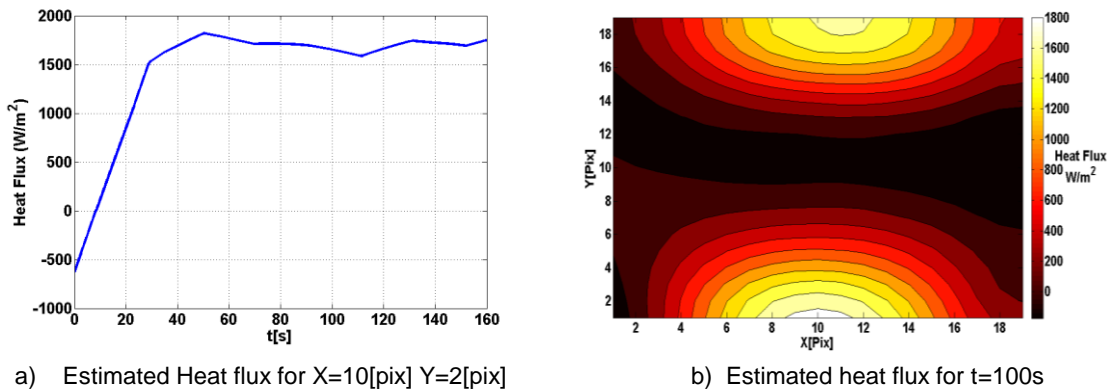


Fig. 10 Estimated heat Flux after 20 iteration

The time domain solution shows a negative heat flux on the initial time that is nonphysical. A uniform temperature was imposed as an initial condition in COMSOL for simplification reasons. Although this was not true on the measured temperature by the infrared camera. For this reason the algorithm finds a heat flux to match such a difference. Discarding the initial seconds, the solution increases from zero in the beginning until it reaches a constant value. The spatial distribution of the heat flux presents the expected distribution, with null value in the central part of the plate and the higher values at the location of the heaters.

The evaluation of the objective function with the iteration number is plotted in figure 11 a). The temperature predicted on surface S1 is compared in figure 11 b), for the same location, with the experimental value obtained with the thermocouple attached on the surface.

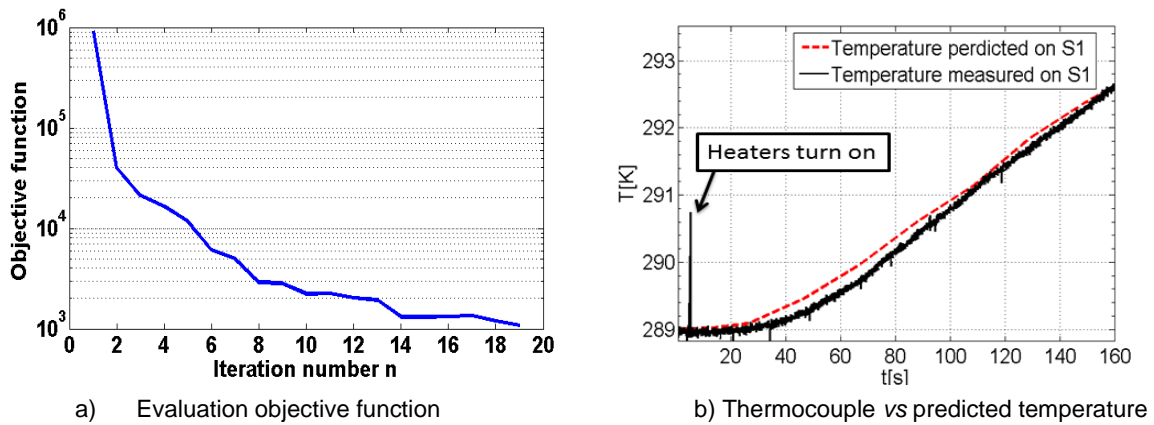


Fig. 11 Verification and validation of the obtained solution

Considering a standard deviation of 0.2K on the infrared measurements, the stopping criteria computed according to Eq.(6) was $2 * 10^3$. This value was reached after the 19 iteration as shown in figure 11a). The estimated temperature distribution on surface S1 is compared with the data obtained with the infrared camera 2 on figure 12.

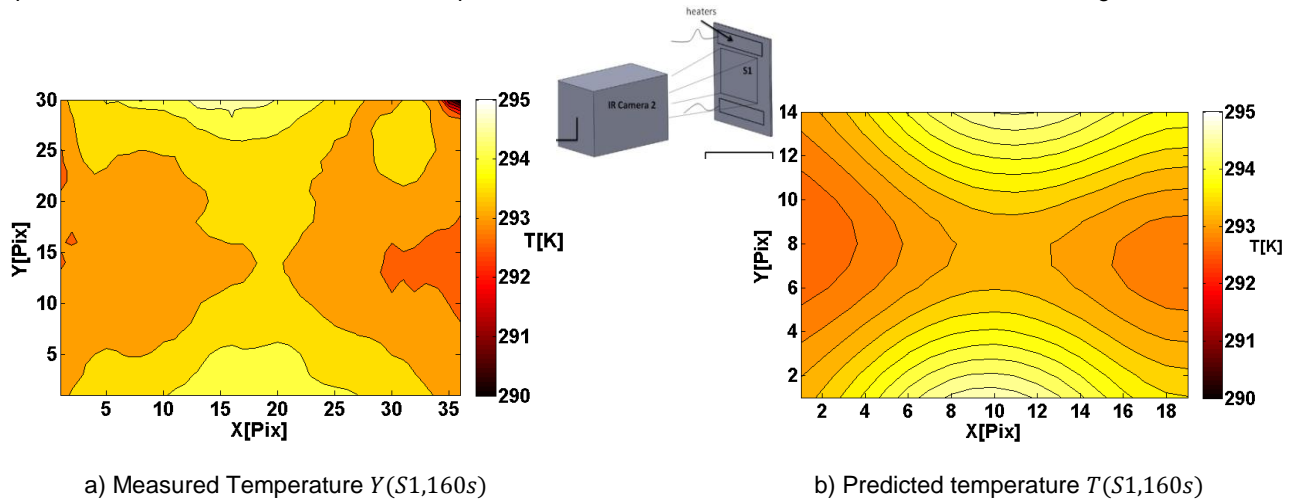


Fig. 12 Comparison between estimated and measured temperature

The resolution of camera 2 was also decreased in order to decrease the noise effects of the infrared image. The estimated temperature distribution shows a similar trend with the measured one. Since it was impossible to compute directly the imposed heat flux such comparison is not performed in the present paper.

5. Conclusion

A comprehensive methodology has been implemented to solve a generalized inverse 3 D heat conduction problem. The method was used to reconstruct the unknown transient heat flux on walls without optical access. The input to the method was provided by the temperature measurements on accessible wall of the same domain by means of infrared thermography. The proposed inverse algorithm was based on conjugate gradient methods and was coupled with a finite element solver *COMSOL*.

The robustness of the implemented method was tested with a numerical study. The influence of measurement noise and dimensionless thickness of the physical domain were analyzed for different cases with uniform and spatial radial heat fluxes distribution. The method shows small influence to measurements noise and its flexibility to solve different physical models.

An experimental validation was performed on a simplified set up. The model was a plate where a heat flux was imposed on one of the surface with electrical heaters. The temperature time series was measured on both sides with two independent infrared cameras. The input for the inverse method was provided by the temperature field on the opposite side of the heaters. The validation was performed by comparing the estimated and measured temperatures on the heaters surface.

Nomenclature

J	gradient direction
P	direction of descent
R	objective function
S	boundary of unknown function
n	iteration number
T	estimated temperature [K]
Y	measured temperature [K]
L	thickness [m]
\dot{L}	dimensionless thickness, $L/3.74\sqrt{\alpha\Delta t}$
Q	heat flux losses [W/m ²]

Greek symbols

β	search step size
γ	conjugate coefficient
ε	convergence criteria
σ	standard deviation of the IR measurements [K]
ξ	dimensionless time, $\alpha t/L^2$
α	thermal diffusivity [m ² /s]

Superscript

· estimated value

REFERENCES

- [1] C. Tropea, A. L. Yarin e J. F. Foss, Handbook of Experimental Fluid Mechanics, Springer, 2007.
- [2] J. V. Beck, B. Blackwell e A. H. Sheikh, "Comparison of some inverse heat conduction methods using experimental data," *Int. J. Heat Mass Transfer*, vol. 39, n.º 17, 1996..
- [3] M. Gradeck, J. Outtara, B. Rémy e D. Maillet, "Solution of an inverse problem in Hankel space - Infrared thermography applied to estimation of a transient cooling flux," *Experimental Thermal and Fluid Science*, vol. 36, pp. 56-64, 2011
- [4] D. Nortershauser, P. Millan, "Resolution of a three-dimensional unsteady inverse problem by sequential method using parameter reduction and infrared thermography measurements" *Numerical Heat Transfer*, vol. 37, p. 587-611, 2000.
- [5] "AVT/VKI Lecture Series: Heat transfer and Inverse Analysis," 2005 EN-AVT-117.
- [6] C. H. Huang., "A three-dimensional inverse heat conduction problem in estimating surface heat flux by conjugate gradient methods," *Int. Jour. of Heat and Mass Transfer*, vol. 42, pp. 3387-3403, 1999.
- [7] M. J. Colaço, H. Orlande e G. S. Dulikravich, "Inverse and Optimization Problems in Heat Transfer," *J. of Braz. Soc. of Mech. Sci. & Eng.*, vol. XXVIII, 2006.
- [8] H. R. B. Orlande, "Inverse Problems in Heat Transfer: New trends on Solution Methodologies and Applications," *Journal of Heat Transfer*, vol. 134, 2012.
- [9] O. M. Alifanov, Inverse Heat Transfer Problems, Springer, 1994
- [10] K. A. Woodbury, Inverse Engineering Handbook, Crc press, 2003.